Neuroimaging Pharmacopoeia

Daniel Thomas Ginat
Juan E. Small
Pamela Whitney Schaefer
Editors

Springer

Neuroimaging Pharmacopoeia

Daniel Thomas Ginat • Juan E. Small
Pamela Whitney Schaefer
Editors

Neuroimaging Pharmacopoeia

Springer

Editors
Daniel Thomas Ginat, MD, MS
Department of Radiology
University of Chicago
Pritzker Medical School
Chicago, IL
USA

Pamela Whitney Schaefer, MD
Department of Radiology
Massachusetts General Hospital
Harvard Medical School
Boston, MA
USA

Juan E. Small, MD
Department of Radiology
Lahey Clinic
Burlington, MA
USA

ISBN 978-3-319-12714-9 ISBN 978-3-319-12715-6 (eBook)
DOI 10.1007/978-3-319-12715-6
Springer Cham Heidelberg NewYork Dordrecht London

Library of Congress Control Number: 2015932672

Printed on acid-free paper

Springer is part of Springer Science+Business Media (www.springer.com)

The authors dedicate this book to the wonderful field or neuroradiology and head and neck imaging, the great advances and discoveries in pharmacology, and to a healthy and (illicit) drug-free world.

Foreword

What you have in front of you is a highly original, different, and useful publication and the only one of its kind in all of diagnostic radiology. The classic definition of "pharmacopoeia" is that of a book containing directions for the identification and preparation of drugs or a list of drugs and their uses. So, in a classic sense, this book is not a pharmacopoeia but something that goes beyond one. Each chapter describes one medication or drug and its indications and action mechanisms, and although in many instances this would suffice to be considered a pharmacopoeia, the authors go further and present a unique and complete series of high-quality neuroimaging studies that reflect the side effects and complications of the drugs discussed. It is, in my opinion, the best and most complete collection of this sort of images that I have even come across, and there is no question that it will be very helpful to neuroradiologists, radiologists, emergency physicians, and many others. Although are shorter than others, all 55 chapters are excellent. Just perusing through the images is fun, eye opening, and informative.

Dr. Schaefer, Small, and Ginat join many of the great, Avicenna, Galen, Vesalius and others who in the past have discussed the use of drugs in pharmacopeias. My recommendations: buy the book- you will not be disappointed, look at the images- you will be entertained, read the book- you will be a better radiologist, and keep the book handy- you will help your patients.

Mauricio Castillo, MD, FACR
Professor of Radiology and Chief of Neuroradiology
University of North Carolina at Chapel Hill
Editor in Chief, American Journal of Neuroradiology
President, American Society of Neuroradiology

Preface

Various medicinal and illicit drugs can result in serious complications affecting the brain, head and neck, and spine. Many of these complications are visible on imaging. In addition, less serious complications or innocuous effects can result in diagnostic conundrums for the imaging interpreter unaware of the patient's drug exposures or their imaging manifestations, while others may produce rather characteristic changes on imaging that should be readily recognized as such. Until now, imaging interpreters have been unable to turn to a dedicated source of information relating to this subject. In this work, we have compiled a fairly comprehensive review of the imaging features of the effects of drugs and pharmaceuticals, from A to Z.

Considering the widespread use of medicinal and illicit drug use throughout the world, familiarity with this subject is critical for the imaging interpreter. Thus, the goal of *Neuroimaging Pharmacopoeia* is to serve as a resource for recognizing these effects and formulating an appropriate differential diagnosis. The term *pharmacopoeia* is derived from the two Greek words *pharmakon* for medicine and *poiein* to make. As such, a pharmacopeia is a compilation of medicinal or pharmacological drugs with their formulas, methods of preparation, effects, and directions of use.

This text represents an adaptation of the classical pharmacopeia, in which each chapter essentially comprises an illustrated pharmacological vignette comprising the indications, mechanism of action, discussion, differential diagnosis, and relevant figures for general classes or specific drugs. Although pharmacology is a dynamic field with perpetual development of new agents, this text provides a fundamental approach for understanding and interpreting neuroimaging studies in patients with drug-induced changes. This knowledge can in turn be used to help optimize patient management in certain cases.

Chicago, IL, USA — Daniel Thomas Ginat, MD, MS
Burlington, MA, USA — Juan E. Small, MD
Boston, MA, USA — Pamela Whitney Schaefer, MD

Acknowledgement

Alaa Jaly, Lancashire Teaching Hospitals
Chris Coutinho, MB, FRCR, Lancashire Teaching Hospitals
Jenny Hoang, MBBS, Duke University
Sachin Mathur, MRCP, FRCR, Lancashire Teaching Hospitals
Gregory Christoforidis, MD, University of Chicago
Alisa Gean, MD, University of California, San Francisco
Christine Glastonbury, MBBS, University of California, San Francisco
Vesna Petronic-Rosic, MD, University of Chicago
Caroline Robson, MBChB, Boston Children's Hospital

Contents

Contributors

Mariam Aboian, MD, Department of Radiology, University of California, San Francisco, CA, USA

Eileen C. Ang, MBBS, Department of Diagnostic Imaging, Monash Medical Center, Monash Health, Melbourne, VIC, Australia

Timothy Biega, MD, Department of Radiology, Tripler Army Medical Center, Honolulu, HI, USA

Maria J. Borja, MD, Department of Radiology, Massachusetts General Hospital, Boston, MA, USA

Ronil V. Chandra, MBBS, MMed, FRANZCR, Department of Diagnostic Imaging, Monash Medical Center, Monash Health, Melbourne, VIC, Australia

Ana M. Franceschi, MD, Diagnostic Radiology, New York University Medical Center, New York, NY, USA

Merav Galper, MD, Department of Diagnostic Radiology, Lahey Clinic, Burlington, MA, USA

Daniel Thomas Ginat, MD, MS, Department of Radiology, University of Chicago, Pritzker Medical School, Chicago, IL, USA

Harut Haroyan, MD, Department of Radiology, University of Chicago, Chicago, IL, USA

Jeffrey Hashim, MD, Department of Diagnostic Radiology, Lahey Clinic, Burlington, MA, USA

Rania Hito, MD, Department of Radiology, University of Massachusetts Memorial Medical Center, Worcester, MA, USA

Grayson W. Hooper, DO, Department of Radiology, Tripler Army Medical Center, Honolulu, HI, USA

Jason M. Johnson, MD, Department of Diagnostic Radiology, MD Anderson Cancer Center, Houston, TX, USA

Kimberly Kallianos, MD, Department of Radiology, University of California, San Francisco, CA, USA

Allan Lee, MBBS, FRANZCR, Department of Diagnostic Imaging, Monash Medical Center, Monash Health, Melbourne, VIC, Australia

Yi Li, MD, Department of Radiology, University of California, San Francisco, CA, USA

William A. Mehan, MD, Department of Radiology, Tufts Medical Center, Boston, MA, USA

Gul Moonis, MD, Department of Radiology, Columbia University, New York, NY, USA

Dee Nandurkar, MBBS, FRANZCR, Department of Diagnostic Imaging, Monash Medical Center, Monash Health, Melbourne, VIC, Australia

Daniel Lopes Noujaim, MD, Department of Diagnostic Radiology, Lahey Clinic, Burlington, MA, USA

Janu Pirakalathanan, MBBS, Department of Diagnostic Imaging, Monash Medical Center, Monash Health, Melbourne, VIC, Australia

Marianne S. Reed, MD, Diagnostic Radiology, Yale University, New Haven, CT, USA

Pamela W. Schaefer, MD, Department of Radiology, Massachussetts General Hospital, Harvard Medical School, Boston, MA, USA

Charles J. Schatz, MD, FACR, Department of Radiology, Beverly Tower Wilshire Advanced Imaging, University of Southern California Keck School of Medicine, Los Angeles, CA, USA

Santosh Shah, MD, Department of Radiology, Massachusetts General Hospital, Boston, MA, USA

Juan E. Small, MD, Department of Diagnostic Radiology, Lahey Clinic, Burlington, MA, USA

Lee-Anne Slater, MBBS, MMed, FRANZCR, Department of Diagnostic Imaging, Monash Medical Center, Monash Health, Melbourne, VIC, Australia

Stephen L. Stuckey, MBBS, MMed, MD, FRANZCR, Department of Diagnostic Imaging, Monash Medical Center, Monash Health, Melbourne, VIC, Australia

Nurhan Torun, MD, Department of Ophthalmology, Beth Israel Deaconess Medical Center, Boston, MA, USA

Michael C. Veronesi, MD, PhD, Department of Radiology, University of Chicago, Chicago, IL, USA

Evan Watkins, MD, Department of Diagnostic Radiology, Lahey Clinic, Burlington, MA, USA

Tobacco

1

Michael C. Veronesi and Daniel Thomas Ginat

1.1 Uses

Although tobacco use is legal, it is not recommended or prescribed for any therapeutic or medicinal purposes. It is smoked or chewed for recreational use as a potent temporary stimulant and mood elevator.

1.2 Mechanism

Nicotine, the primary active compound in cigarettes, is considered one of the most addictive of all substances because of its rapid onset and offset effects on the brain's dopamine reward systems. Inhaled nicotine can distribute in the brain within 10 s of inhalation but lasts mere seconds, causing a powerful urge for more. Of note, the long-term devastating sequela from smoking as it relates to neurologic disease are only partially explained by nicotine. Aside from nicotine, tobacco contains over six thousand other chemical compounds. In particular, polycyclic aromatic hydrocarbons and the tobacco-specific nitrosamine 4-(methylnitrosamino)-1-(3-pyridyl)-1-butanone have been implicated as the major carcinogens associated with cigarette smoking. Additional details regarding the mechanisms of action for specific conditions are discussed in subsequent sections.

M.C. Veronesi, MD, PhD
Department of Radiology, University of Chicago, Chicago, IL, USA

D.T. Ginat, MD, MS (✉)
Department of Radiology, University of Chicago, Pritzker Medical School, Chicago, IL, USA
e-mail: ginatd01@gmail.com

1.3 Discussion

Tobacco use is the leading cause of preventable death in the United States. An estimated 400,000 deaths or nearly one of every five deaths in the United States is associated with adverse conditions caused by smoking each year. Nearly every organ system is affected by cigarette smoking. The associated manifestations of cigarette smoking from a neuroimaging standpoint include the direct link between smoking and large vessels and lacunar infarcts, chronic small vessel ischemic disease, cerebral aneurysms, cerebral venous thrombosis, head and neck cancer of the squamous type, lung cancer metastases to the brain, and Warthin tumors.

1.3.1 Stroke

Compared with nonsmokers, cigarette smoking is estimated to increase the risk of stroke by 2–4-fold. Of note, stroke is the third leading cause of death in the United States with significant comorbidity in survivors. Mechanisms by which primary and second-hand tobacco smoke exposure increase the risk of stroke and heart disease

D.T. Ginat et al. (eds.), *Neuroimaging Pharmacopoeia*,
DOI 10.1007/978-3-319-12715-6_1, © Springer International Publishing Switzerland 2015

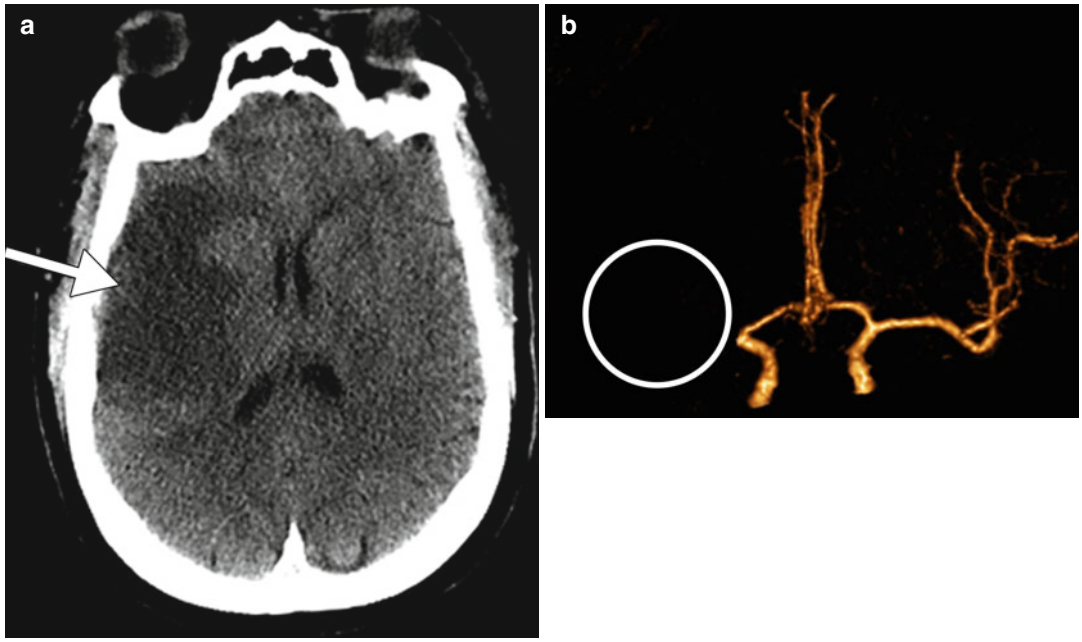

Fig. 1.1 Embolic infarct. This smoker presented with acute left hemiplegia. Non-contrast axial CT image (**a**) shows a hypoattenuation within the right MCA territory (*arrow*). 3D CTA image (**b**) shows occlusion of the right MCA (expected location *encircled*)

include carboxyhemoglobinemia, increased platelet aggregation, increased fibrinogen levels, reduced HDL cholesterol, and direct toxic effects of compounds such as 1,3-butadiene, a vapor phase constituent of environmental tobacco smoke that has been shown to accelerate atherosclerosis. Indeed, atherosclerosis and formation of both occlusive and embolic thrombi are the major causes of cerebrovascular accidents. Smoking is also associated with lacunar infarcts and chronic small vessel ischemic disease. Smoking cessation results in a considerable reduction in stroke risk.

On conventional angiography, CTA or MRA, atherosclerosis manifests as luminal narrowing that may be associated with calcifications. Acute embolic thrombus is suggested by intraluminal high attenuation on non-contrast CT, such as the hyperdense MCA sign, and manifests as an abrupt termination of the artery with absence of flow distally on CTA, MRA, or conventional angiography (Figs. 1.1). Hyperacute infarcts are often unapparent on non-contrast CT, but acute and early subacute infarcts can appear as areas of hypoattenuation with loss of gray white matter differentiation and swelling. MRI with diffusion-weighted imaging is more sensitive for detecting early infarcts, which appear as areas of high T2 signal and restricted diffusion (Fig. 1.2). Besides smoking, other causes and risk factors for stroke include hypertension, hypercholesterolemia, diabetes, use of other drugs, such as cocaine and amphetamines (refer to Chaps. 5 and 6), dissection (Fig. 1.3), and vasculitis, such as lupus or Takayasu arteritis (Fig. 1.4). In addition to large territorial infarcts, smokers are prone to more extensive small vessel ischemic disease, which can manifest as areas of high T2 signal in the cerebral white matter (Fig. 1.5).

1.3.2 Cerebral Aneurysm

Besides smoking, additional risk factors that predispose to aneurysm formation include fenestrated arteries (Fig. 1.6), fibromuscular dysplasia, neurofibromatosis, alpha-1-antytripsyn deficiency, and

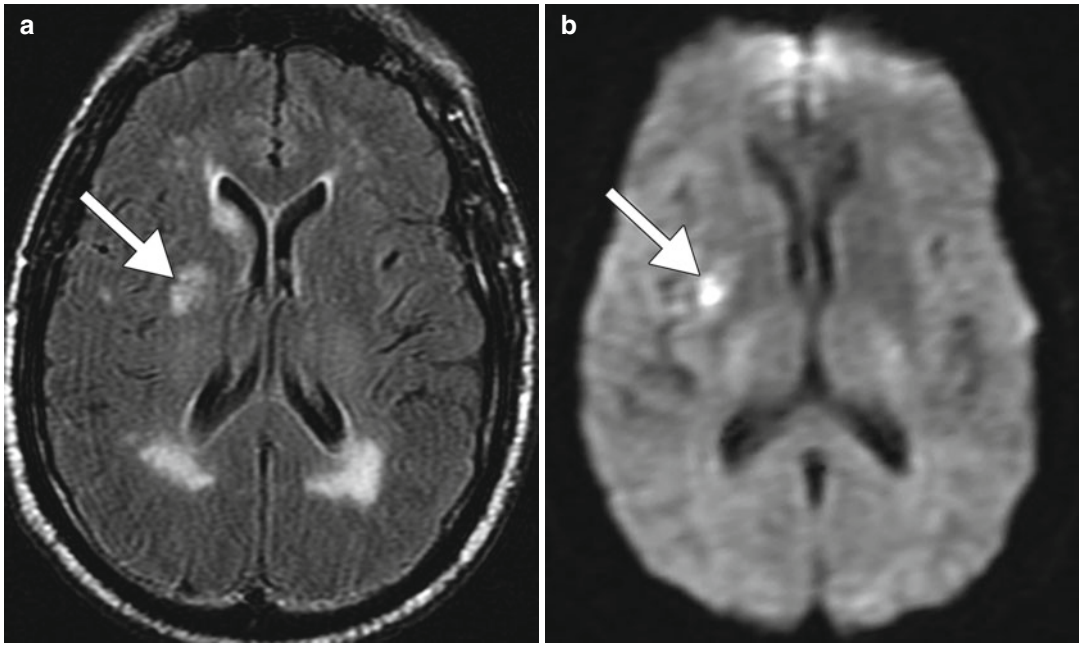

Fig. 1.2 Lacunar infarct and small vessel ischemic disease. The patient is a smoker who presented with acute neurological deficits. Axial FLAIR (**a**) and DWI (**b**) images show a recent right basal ganglia lacunar infarct (*arrows*). There is also diffuse, confluent periventricular white matter T2 hyperintensity as well as mild scattered, punctate subcortical white matter T2 hyperintense foci without corresponding restricted diffusion, which is consistent with chronic small vessel ischemic disease

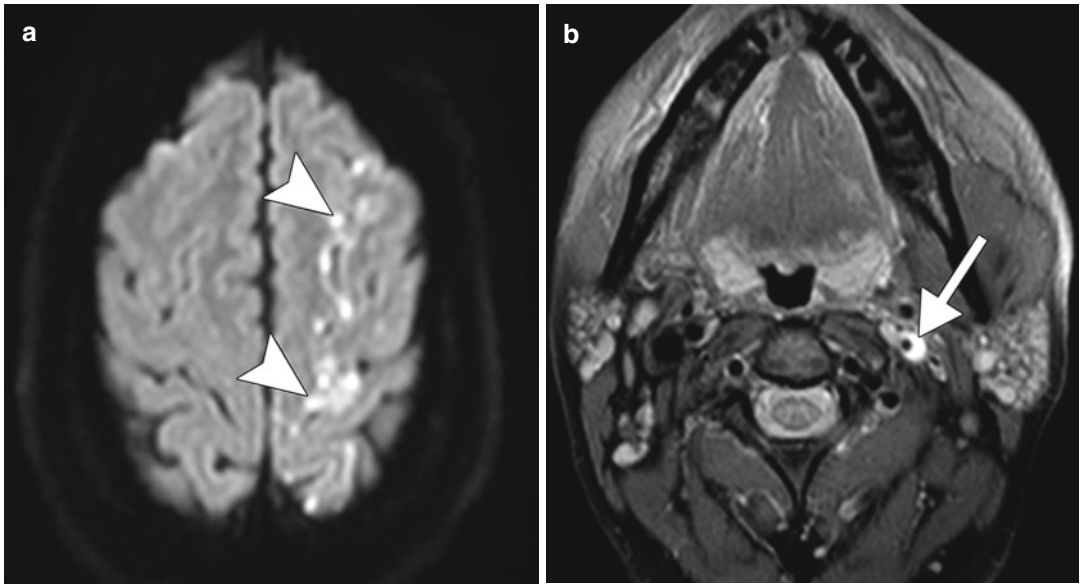

Fig. 1.3 Carotid dissection. Axial DWI (**a**) shows restricted diffusion in the left ACA-MCA watershed territory (*arrowheads*). The axial fat-suppressed T1 MRA (**b**) shows hyperintensity surrounding the narrow left internal carotid artery flow void, compatible with intramural hemorrhage (*arrow*)

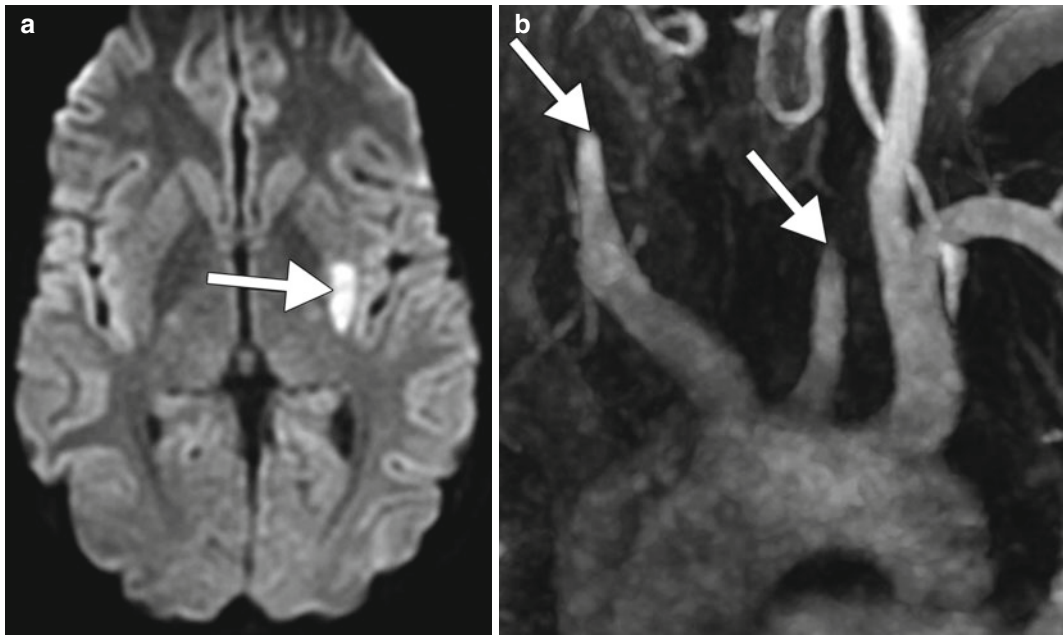

Fig. 1.4 Takayasu arteritis. Axial DWI (**a**) shows a focus of restricted diffusion in the left external capsule (*arrows*). MIP MRA (**b**) shows lack of flow-related enhancement beyond the proximal common carotid arteries bilaterally (*arrows*)

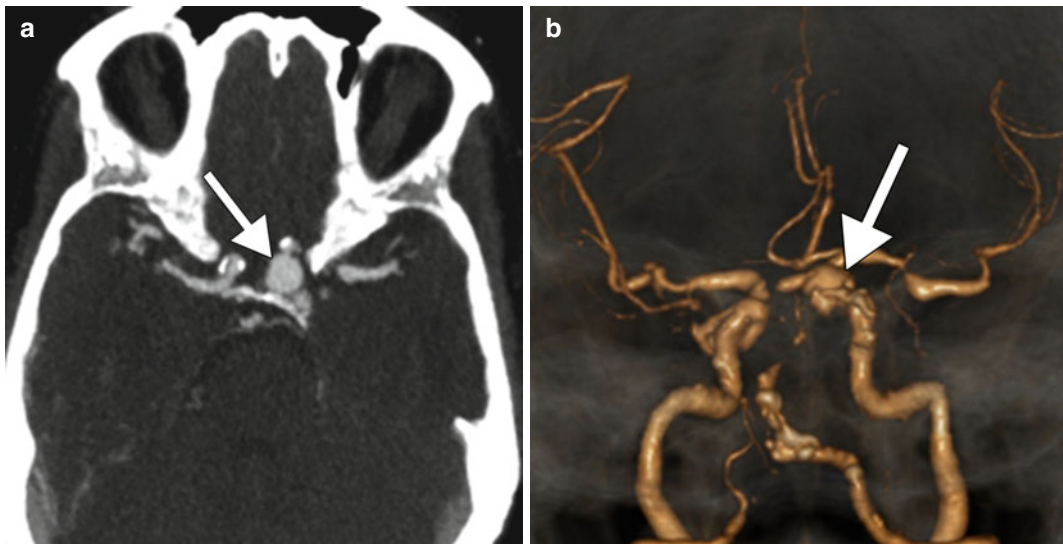

Fig. 1.5 Cerebral aneurysm. A former 20-pack-year smoker underwent evaluation for a suspected stroke. Axial (**a**) and 3D volume rendered (**b**) CTA images show a left paraclinoid internal carotid artery saccular aneurysm (*arrow*). There is also extensive atherosclerotic narrowing of the cerebral vasculature noted in both the anterior and posterior circulation bilaterally

connective tissue disorders, such as Ehlers-Danlos syndrome and Marfan's syndrome and polycystic kidney disease. Otherwise, the differential diagnosis of a cerebral aneurysm on radiologic imaging includes an infundibulum (usually manifests as a triangular dilatation with the vessel arising from the apex that measures less than 2 mm), pseudoaneurysm, and mycotic aneurysm (Fig. 1.7).

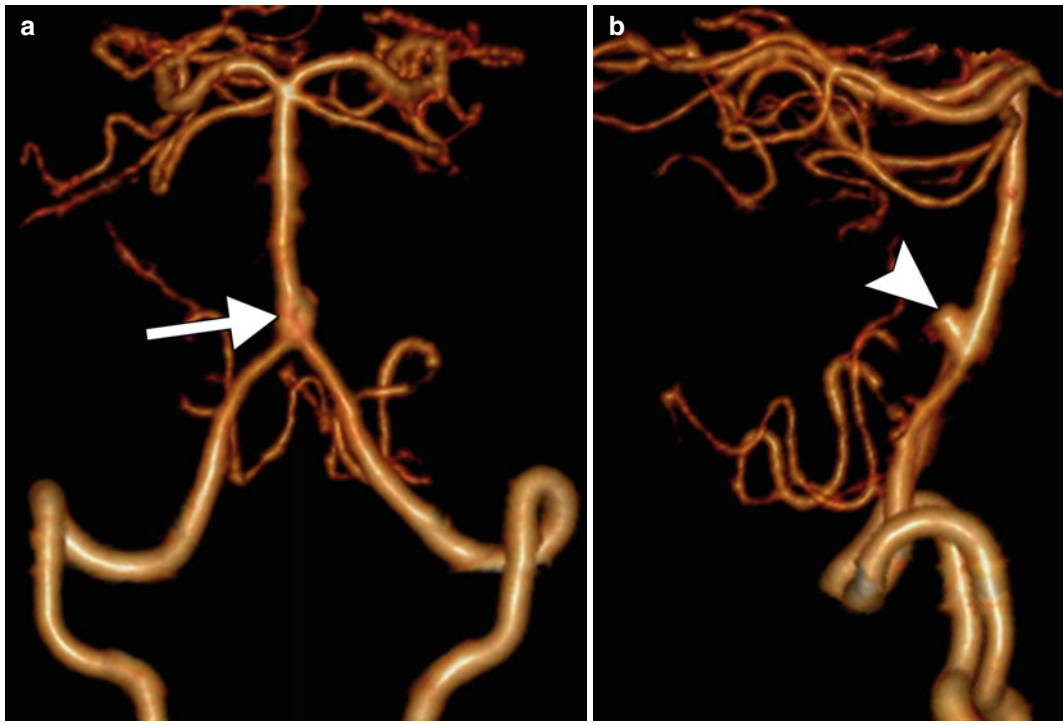

Fig. 1.6 Arterial fenestration. Frontal projection 3D volume rendered CTA image (**a**) shows a fenestration of the proximal basilar artery (*arrow*). Lateral projection 3D volume rendered CTA image (**b**) shows a dorsally oriented aneurysm arising from the caudal aspect of the fenestration (*arrowhead*)

1.3.3 Cerebral Venous Thrombosis

Secondary polycythemia due to chronic smoking is a risk factor developing cerebral venous thrombosis. Refer to the L-asparaginase and oral contraceptives chapters (Chaps. 21 and 47) for examples of venous thrombosis on imaging.

1.3.4 Head and Neck Cancer, Squamous Cell Carcinoma

Tobacco smoking, along with alcohol, is well established as the dominant risk factor for head and neck squamous cell carcinoma (HNSCC). This risk is correlated with the intensity and duration of tobacco use and is synergistic with concomitant alcohol consumption. There are more than sixty recognized compounds in tobacco that have a specific carcinogenic potential. In particular, nitrosamines and polycyclic hydrocarbons can alter the molecular profile of an individual and causes mutations. Nicotine, originally thought only to be responsible for tobacco addiction, is also involved in tumor promotion and progression with antiapoptotic and indirect mitogenic properties. Other factors that can increase the risk of HNSCC include HPV infection and certain occupational exposures. Imaging with contrast-enhanced CT and MRI allows depiction of the anatomy of the larynx and submucosal tumor extension.

Dual-energy CT improves the diagnostic performance and interobserver reproducibility of evaluations of laryngeal cartilage invasion by squamous cell carcinoma. CT, MRI, and PET-CT also provide information regarding cervical nodal disease, systemic metastases, and synchronous malignancies.

On CT or MRI, head and neck squamous cell carcinomas often manifest as ill-defined enhancing masses. Aggressive features of

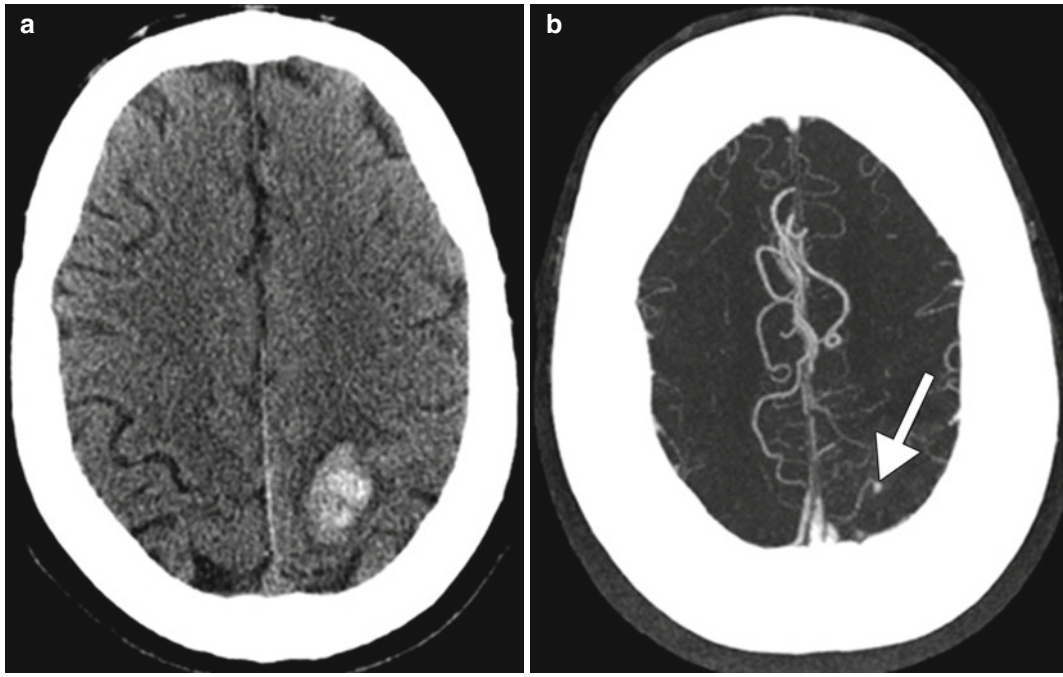

Fig. 1.7 Mycotic aneurysm. Axial CT image (**a**) shows left peri-rolandic hemorrhage. Axial MIP CTA image (**b**) shows a small outpouching arising from a cortical artery (*arrow*)

HNSCC include tissue invasion and necrosis (Fig. 1.8). The most common sites of head and neck squamous cell cancer are the floor of the mouth, tongue, soft palate, anterior tonsillar pillar, and retromolar trigone. In addition to locoregional spread, HNSCC can metastasize to distant organs hematogenously, most commonly to the lungs and bones. Metastasis to the brain is an infrequent, but carries a poor prognostic outcome (Fig. 1.9). Besides smoking, alcohol (refer to Chap. 2), betel nuts (refer to Chap. 8), and HPV are the other major risk factors for head and neck squamous cell carcinoma. Interestingly, HPV-positive squamous cell carcinomas generally have a more favorable prognosis and tend to have tumors that are relatively well-defined and large cystic nodal metastases (Fig. 1.10). Otherwise, the differential for other malignant cancers in the head and neck include thyroid cancer, lymphoma, salivary gland cancer, and sarcoma. Furthermore, head and neck abscesses can sometimes resemble necrotic or ulcerated head and neck squamous cell carcinomas and nodal metastases (Fig. 1.11).

1.3.5 Brain Metastases

In addition to HNSCC, smoking has been shown to be a risk factor for the formation of several other types of cancers, including lung cancer, acute myeloid leukemia, bladder cancer, cervical cancer, renal cancer, esophageal cancer, gastric cancer, pancreatic cancer, and colorectal cancer. The majority of these cancers have at least some potential for metastasizing to the brain, which is the most feared complication of systemic malignancies. If no one smoked, one of every three cancer deaths in the United States would be avoided. Lung cancer has the highest association with smoking, causing an estimated 90 % of all lung cancer deaths in men and 80 % of all lung cancer deaths in women, and is the most common cancer that metastasizes to the brain. Nicotine-derived nitrosamine ketone (NNK) has

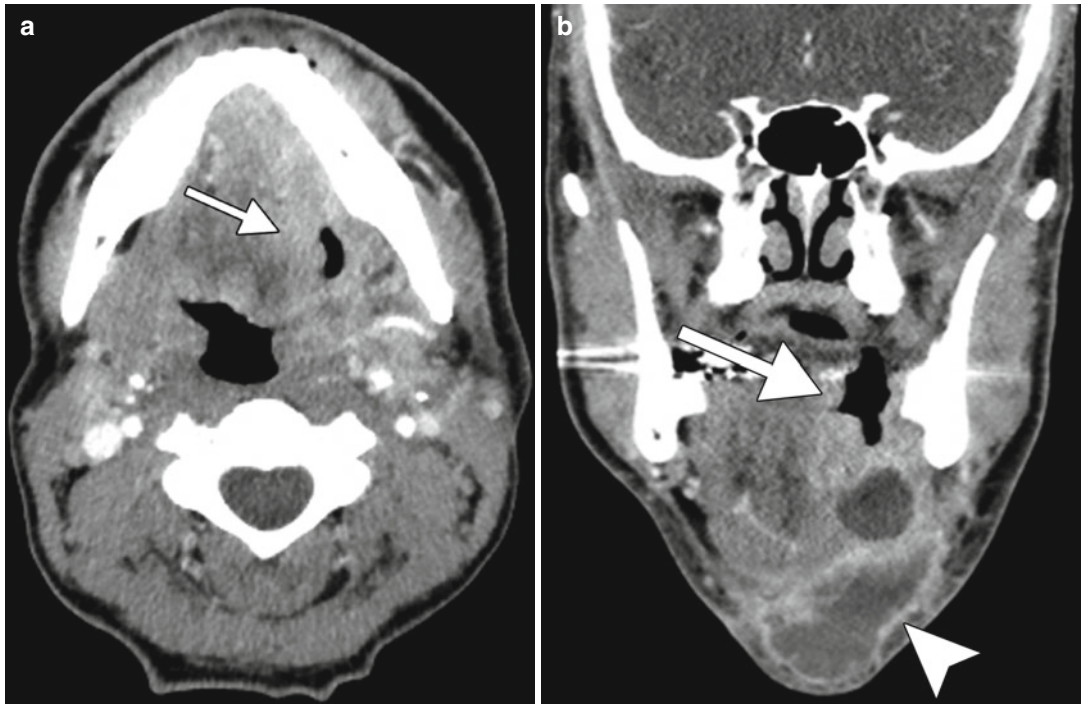

Fig. 1.8 Oral squamous cell carcinoma in a 30-pack-year male smoker. Axial (**a**) and coronal (**b**) post-contrast CT images show an ulcerating mass in the left floor of the mouth and oral tongue (*arrows*) with associated submental necrotic cervical lymphadenopathy (*arrowhead*)

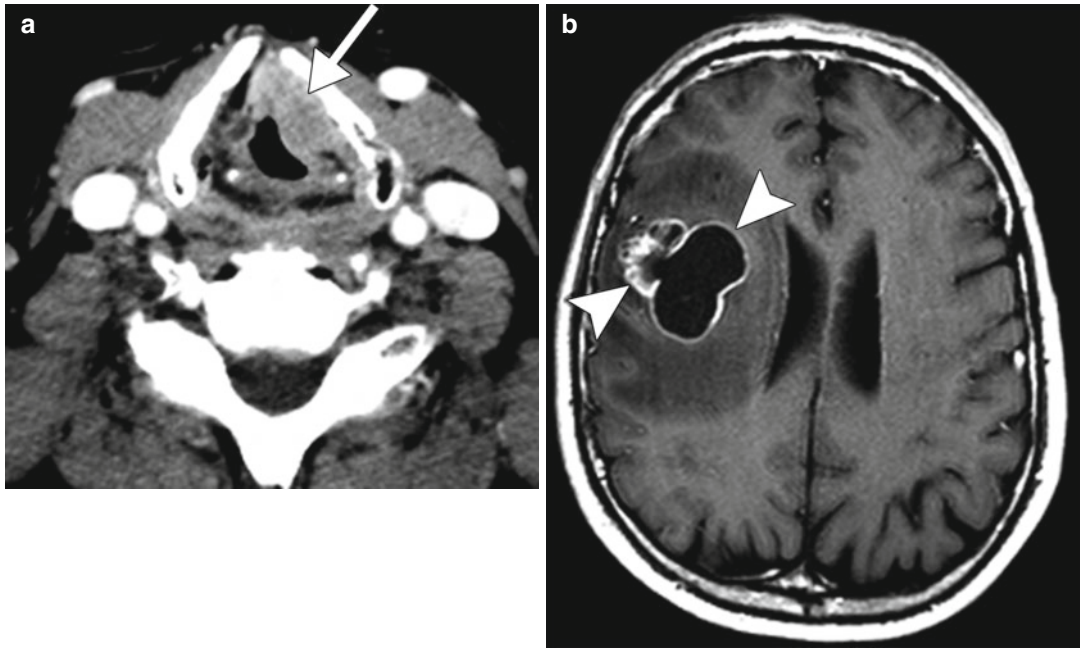

Fig. 1.9 Laryngeal squamous cell carcinoma with brain metastasis. This 25-pack-year smoker had been recently diagnosed with laryngeal squamous cell carcinoma when he developed generalized seizures. Axial CT image (**a**) shows a left vocal cord mass (*arrow*) that also involves the paraglottic fat and anterior commissure. Post-contrast T1-weighted MRI image (**b**) demonstrates a heterogeneous metastatic lesion in the right frontal lobe (*arrowheads*)

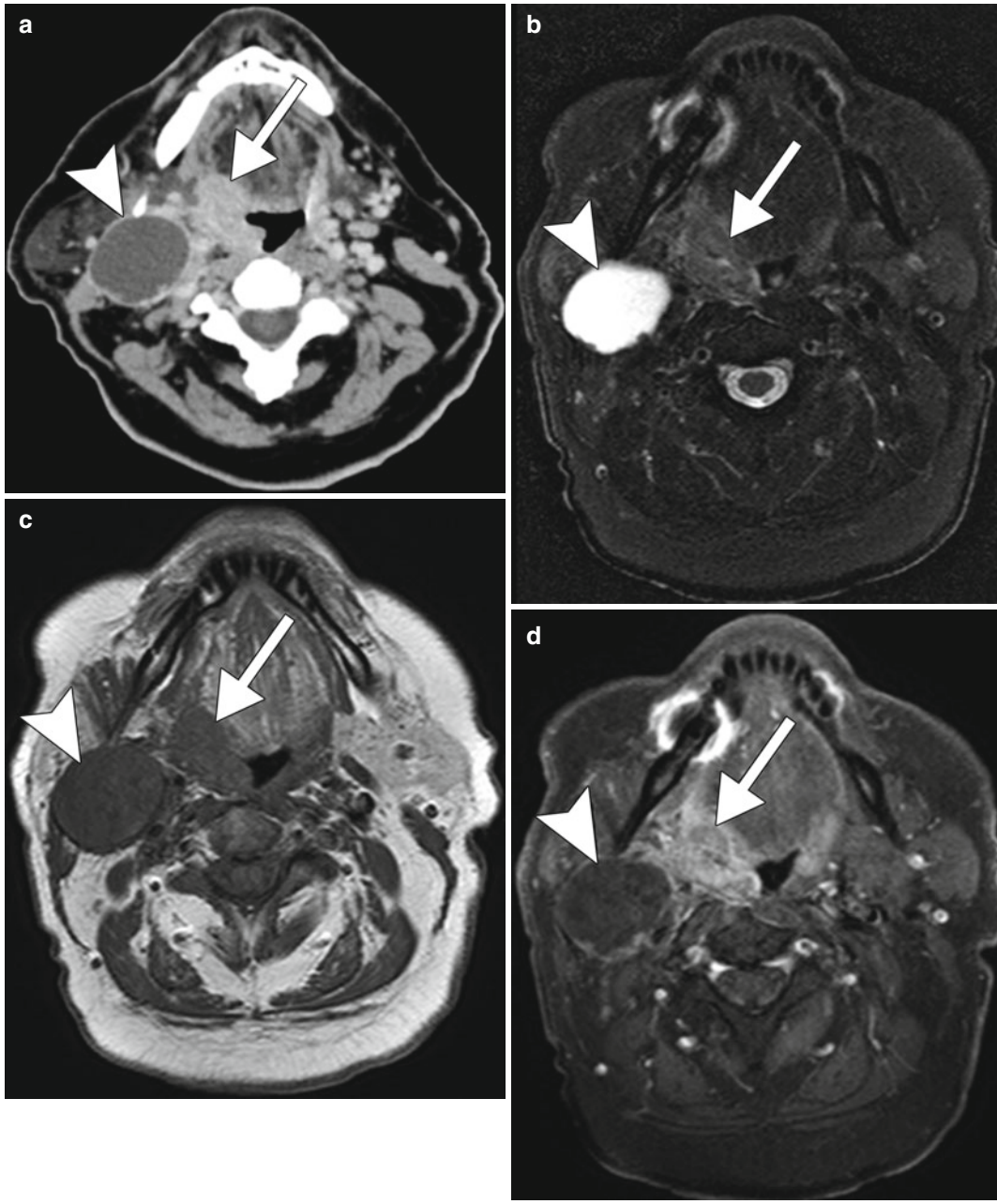

Fig. 1.10 HPV-positive squamous cell carcinoma. Axial CT (**a**) and axial fat-suppressed T2-weighted (**b**), axial T1-weighted (**c**), and axial fat-suppressed post-contrast T1-weighted (**d**) images show a relative well-demarcated right palatine tonsil tumor (*arrows*) and a large metastatic lymph node with cystic necrosis (*arrowheads*)

been identified as a potent procarcinogen specific to the development of lung cancer. The two categories of lung cancer metastases to the brain consist of small cell lung carcinoma (Fig. 1.12) and non-small cell lung carcinoma (NSCLC), such as adenocarcinoma (Fig. 1.13). MRI with contrast is the gold standard for evaluation of brain metastases. Lung cancer metastases to the brain are typically iso- to hypointense on T1 and hyperintense on T2-weighted sequences. The

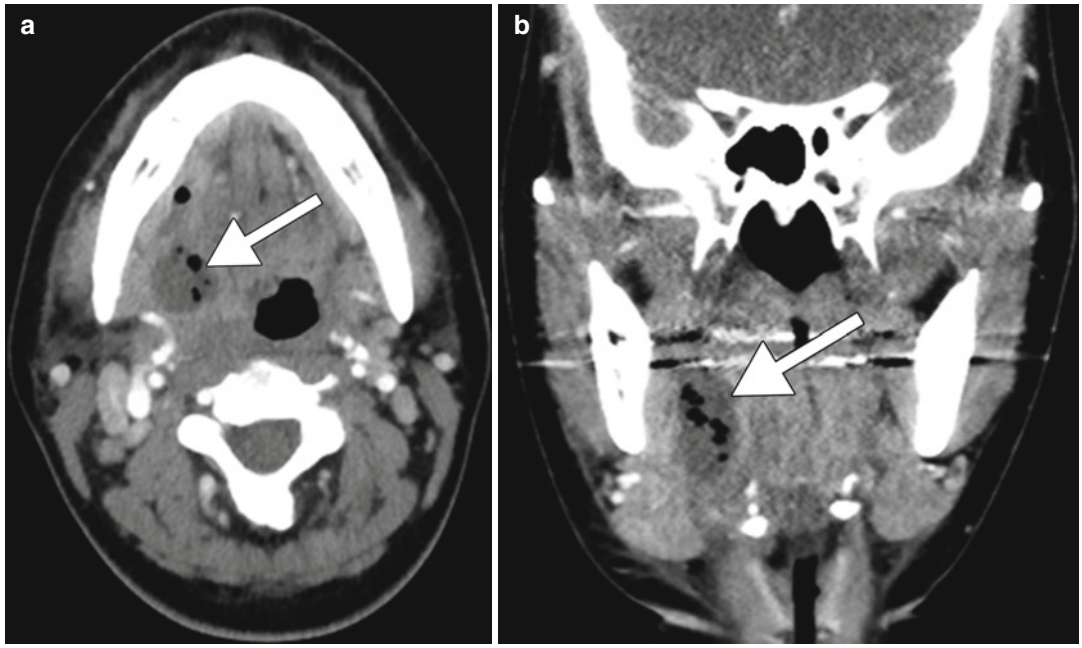

Fig. 1.11 Floor of mouth abscess. Axial (**a**) and coronal (**b**) post-contrast CT images show a fluid collection with internal air in the right floor of the mouth (*arrows*) in a patient with mouth pain and fever

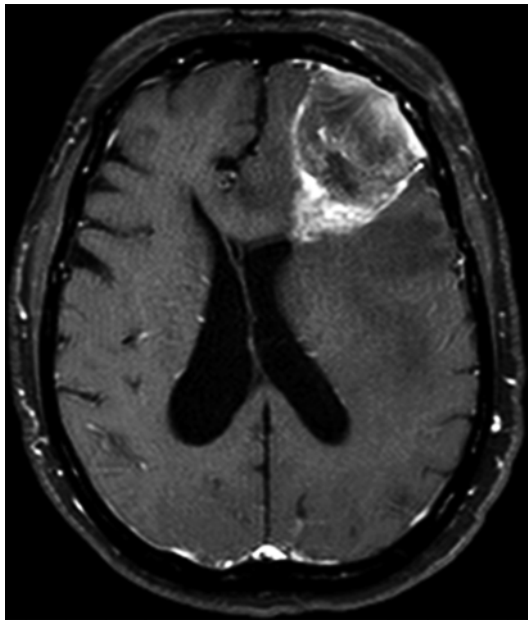

Fig. 1.12 Small cell lung carcinoma metastasis to the brain. The post-contrast T1-weighted MRI in a 40-pack-year smoker who presented with a 2 weeks history of aphasia, forgetfulness, and frequent falls shows a heterogeneously enhancing mass within the left frontal lobe with associated subfalcine herniation

Fig. 1.13 Non-small cell lung cancer brain metastases. The patient has a 40-pack-year smoking history, and known small cell lung cancer metastases to the bone developed altered mental status and intermittent left-sided weakness. The axial post-contrast T1-weighted MRI shows ring-enhancing lesions in the right cerebral hemisphere and a smaller solidly enhancing lesion in the left frontal lobe (*arrow*)

enhancement pattern is usually intense whether uniform, punctate, or ring enhancing. Hemorrhagic lung metastases may display high intrinsic T1 signal. On T2-weighted sequences, metastatic lesions are typically hyperintense with hyperintense peritumoral edema. On MR spectroscopy, there is often an intratumoral choline peak without choline elevation in the peritumoral edema and depletion of NAA. CT may be the initial exam obtained when metastatic disease is not yet known. On precontrast imaging, the mass may be iso- to hypoattenuating, surrounded by variable amounts of vasogenic edema. Similar to MRI, following administration of contrast in CT, enhancement is variable and can be intense, punctate, nodular, or ring enhancing. It is also important to evaluate the skull, soft tissues, and head and neck lymph nodes for additional metastases.

The differential diagnosis for brain metastases includes primary brain tumors (Fig. 1.14), cerebral abscess (refer to Chaps. 7, 16, 19, and 46), focal subacute stroke, and tumefactive demyelinating lesions.

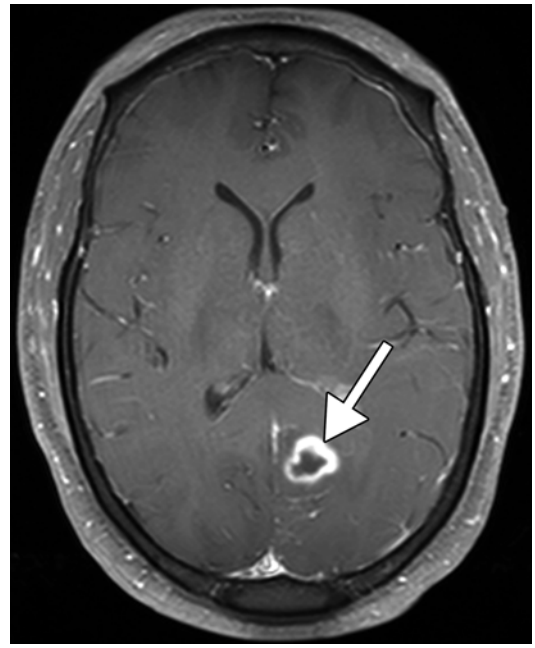

Fig. 1.14 Glioblastoma. Axial post-contrast T1-weighted MR image shows a ring-enhancing mass centered in the left posterior cingulate gyrus (*arrow*)

1.3.6 Warthin Tumor

Papillary lymphomatous cystadenoma of the parotid gland, or Warthin tumor, is significantly associated with a history of cigarette smoking. Indeed, over 90 % of Warthin tumors occur in tobacco smokers. The tumor arises almost exclusively in the parotid gland and has a predilection for male Caucasians. These lesions most commonly present as asymptomatic masses, but may cause facial nerve paralysis or tinnitus. Warthin tumors consists of oncocytic cells containing numerous mitochondria frequently showing structural abnormalities and reduced metabolic function. Smoking can lead to damage to mitochondrial DNA due to the development of numerous reactive oxygen species. In this context, a high rate of deleted mitochondrial DNA has been detected in the oncocytic cells of Warthin tumor. Typical imaging features consist of well-defined solid and/or cystic masses usually within the inferior pole (tail) of the parotid gland, not infrequently multifocal and bilateral (Fig. 1.15).

The differential diagnosis of Warthin tumor includes non-neoplastic conditions, such as benign lymphoepithelial lesions, Sjogren syndrome, and sarcoidosis. For example, benign lymphoepithelial lesions are typically associated with HIV and classically appear as multiple bilateral cystic parotid masses that may contain solid components (Fig. 1.16). Warthin tumors can also resemble pleomorphic adenomas on imaging. However, pleomorphic adenomas are less likely to occur in the parotid tail and display a bosselated appearance and high T2 signal on MRI (Fig. 1.17). While clinical history may be helpful in differentiating some of these possibilities, predictive features of malignancy on imaging include T2 hypointensity of the parotid, ill-defined margins, diffuse growth, infiltration of subcutaneous tissue,

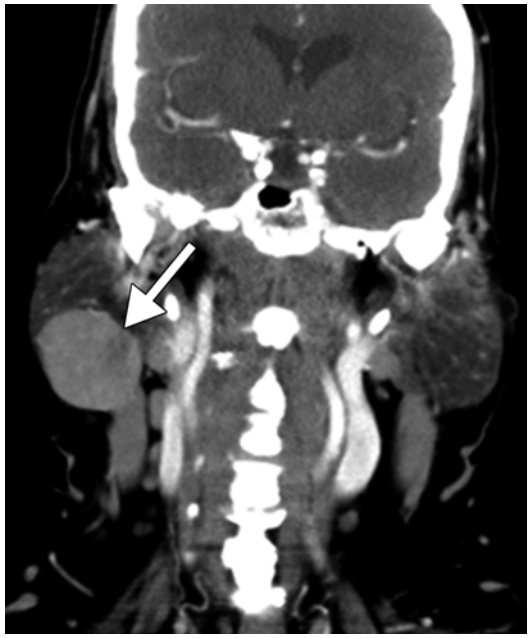

Fig. 1.15 Warthin tumor. This smoker with COPD presented with growing right-sided neck mass. The coronal post-contrast CT image shows a well-defined hyperattenuating mass within the right parotid tail (*arrow*)

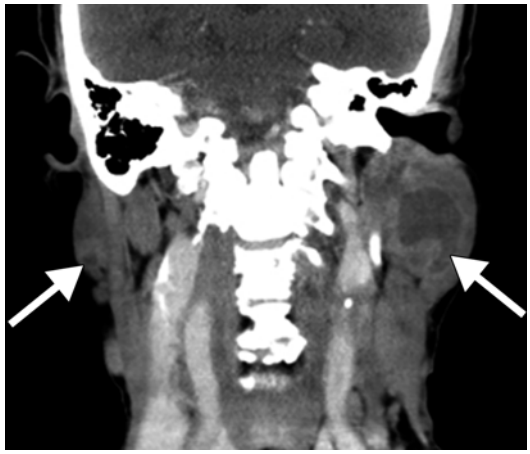

Fig. 1.16 Benign lymphoepithelial lesions in a patient with HIV. The coronal CT image shows cystic lesions in the bilateral parotid glands (*arrows*). The lesion on the left side contains a solid nodule

lymphadenopathy, and perineural spread (Fig. 1.18). However, Warthin tumors often demonstrate T2 hypointense foci and low ADC values and thus cannot be reliably differentiated from many malignant tumors on diffusion-weighted imaging. In addition, Warthin tumors typically display marked hypermetabolism on ^{18}FDG-PET.

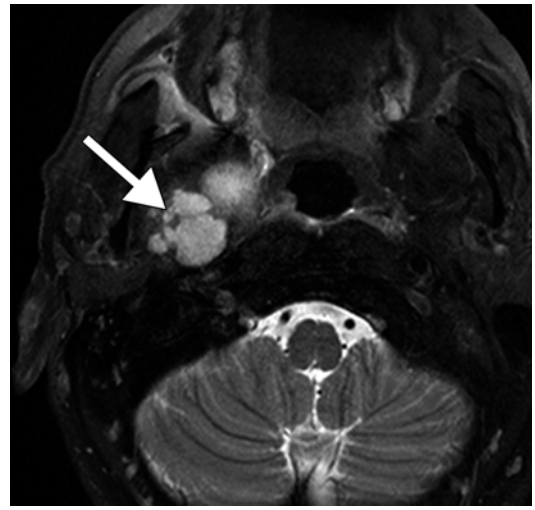

Fig. 1.17 Parotid pleomorphic adenoma. Axial fat-suppressed T2-weighted MRI shows a bosselated T2 hyperintense mass arising from the deep lobe of the right parotid gland (*arrow*)

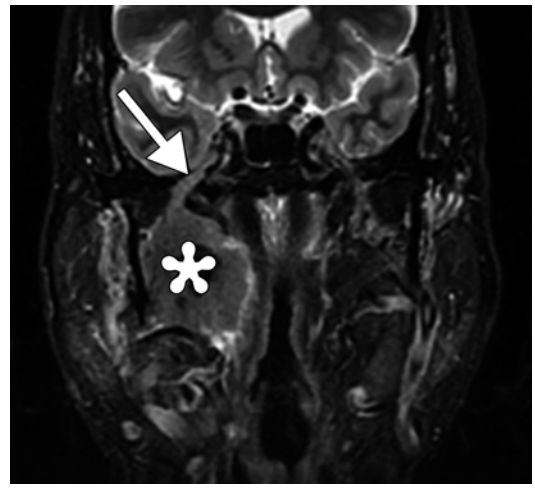

Fig. 1.18 Parotid pleomorphic adenocarcinoma. The coronal STIR MRI shows a heterogeneous mass arising from the deep lobe of the parotid gland (*) with perineural extension along the mandibular nerve across the foramen ovale (*arrow*)